A new investigation used to predict the burst pressure in straight corroded pipes under internal pressure

Aicha Metehri[a], *Belaïd* Mechab[b], *Bel Abbes* Bachir Bouiadjra[c]

University of Sidi Bel Abbes, Faculty of Technology,
Mechanical Engineering Department,
Laboratory of Physical Mechanics of Materials,
Sidi Bel Abbès, People's Democratic Republic of Algeria

[a] e-mail: ametehri@yahoo.com, **corresponding author**,
   ORCID iD: https://orcid.org/0009-0002-2221-6833

[b] e-mail: bmechab@yahoo.fr,
   ORCID iD: https://orcid.org/0009-0000-7483-5527

[c] e-mail: bachirbou@yahoo.fr,
   ORCID iD: https://orcid.org/0000-0002-1925-7194

Abstract:

Introduction/purpose: There is a growing interest in pipeline integrity and its effects on economic and safety aspects. This study examines the process of corrosion evaluation in order to identify the remaining structural integrity of thin-walled pipelines with corrosion problems.

Methods: This work aims to create a corrosion evaluation model that can analyse the deterioration of steel pipes caused by internal pressure. A study utilised the finite element approach to build models for predicting the burst pressure of defect-free straight pipes. The study involved analytical and numerical analysis and used the mathematical extrapolation method.

Results: This paper discusses the impact of several factors on the integrity of a pipe, including the depth of defects, the thickness of the pipe, the shape, the size, and the position of faults, as well as the interaction between internal and external defects. Additionally, the influence of external defects on the overall integrity is discussed.

Conclusion: It is concluded that the pipeline corrosion failure criterion (PCORRC) model and the presented model align with the analytical solution documented in the literature. This holds immense importance in the field of structural design and safety evaluation.

Keywords: corrosion defect, steel pipe, internal pressure, failure, stress, modelling.

Introduction

Pipelines are pivotal components of the energy infrastructure, facilitating the cost-effective transportation of gas, oil, and various hydrocarbons across extensive distances to fulfil the requirements of the petrochemical sector (Mechab et al, 2011, 2014).

Pipeline integrity management adopts a performance-oriented strategy aimed at guaranteeing the operational reliability of pipelines and averting potential failures, with careful consideration given to the hazardous properties of the transported substances (Mechab et al, 2018, 2020; Fezazi et al, 2021; Salem et al, 2019). This comprehensive process comprises pipeline inspection, integrity evaluation, and maintenance tasks, with inspections to detect anomalies like corrosion defects and cracks (Guidara et al, 2018; Amaya-Gómez et al, 2019; Muthanna et al, 2021). Corrosion emerges as a leading cause of deterioration in pipelines, marked by the gradual erosion of metal over time, often detected through in-line Inspections (Deng et al, 2021; Jiang & Zhao, 2022). The corrosion observed on pipelines displays a range of shapes. Categorised by these shapes, corroded pipelines can be grouped into three main types: single-point corrosion defects, multi-point corrosion defects, and complex corrosion defects (Zhao et al, 2022; Teohet al, 2022; Yeomet al, 2015; Yi et al, 2022; Zelmati et al, 2020).

Over time, predictive models targeting the estimation of burst pressure in cylindrical vessels and pipes have evolved. They seek to quantify the maximum failure pressure by considering material properties, diameter, and wall thickness (Wang et al, 2020; Zhuwu et al, 2020). Numerous prediction models have been developed for determining burst pressure in pipes with isolated surface defects, mainly focusing on materials exhibiting elastic/ideally plastic behaviour (Abyani et al, 2022; Zhou et al, 2021).

Present models used to forecast the burst pressure of pipes with surface corrosion defects, utilising finite element analysis (FEA), generally presuppose defects to be axially oriented and either elliptical or rectangular (Kiefner et al, 1973) as per (DNV, 2021); elliptical shapes are assumed for shorter defects, whereas longer ones are deemed rectangular. Conversely, an alternative reference (ASME, 2012) posts an arbitrary defect profile aligned with the axis. Rectangular defect geometry

is uniformly employed in all other current FEA-based models for predicting burst pressure in such pipes.

This study aims to develop a corrosion assessment model to analyse damage in pipes under internal pressure. The finite element method is used to diagnose a corrosion defect in a steel pipe. The effect of the depth of the defect, the thickness of the pipe, the shape, the size, the position, the interaction between internal and external defects, and the external defect associated with a higher risk is discussed in this work. The new model presented in this paper predicts the burst pressure of a defect-free straight pipe, which is of great significance to structural design and safety assessment.

Numerical modeling and FE

In this case, the primary structure analysed is a three-dimensional structure. The ABAQUS calculation software (Hibbitt, Karlsson & Sorensen, 2014) was used in the present work to obtain the equivalent circumferential, radial, and longitudinal stress fields generated in a pipeline bearing a centred square external defect.

Geometrical and materials models

In this study, the defect is located in the central square outer wall of the pipe, and the dimensions of the defect length, width, and depth are a=40mm, b=40mm, and c=4 mm, respectively. Figure 1 shows the geometrical characteristics of the corroded pipe and different paths of study. It is worth noting that the external diameter is R_{ext}, R_{int} is the inner diameter, L is the longitudinal length, and ''t'' is the thickness of the pipe, as shown in Table 1. The tube material is API 5L X65 steel. This pipe was subjected to internal pressure.

Table 1 – Geometrical structure dimensions

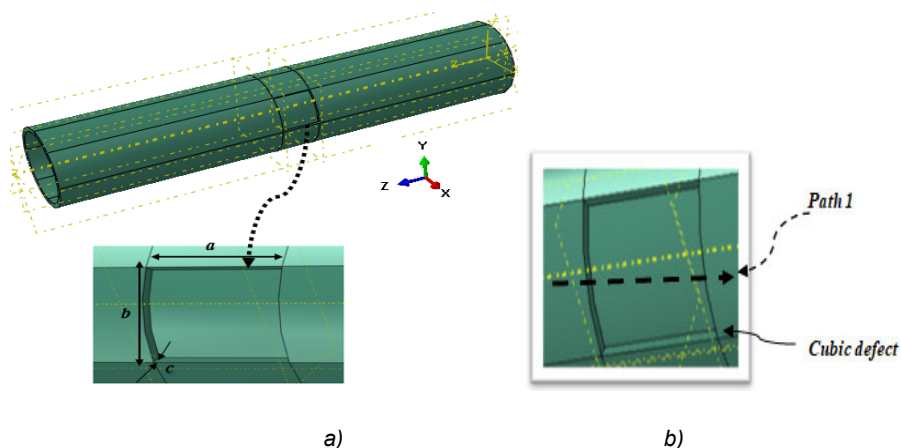| t(mm)	L(mm)	R_{ext} (mm)	R_{int} (mm)	P (MPa)
5mm	500mm	50	45	10-15-20

a)   *b)*

Figure 1 – a) Geometrical characteristics of the corrosion defect, b) Path of study

Table 2 presents the mechanical properties of the material used in this study (Olusegun & Akid, 2014).

Table 2 – API 5L X65 steel mechanical properties

Material	5L X65
Young's modulus E (GPa)	211
Poisson ratio ν	0.3
n (work hardening coefficient)	0.127
σ_{uits} [MPa]	500
σ_e [MPa]	380

Initial conditions and limitation

Boundary conditions are necessary for any finite element calculation. A section of steel pipe was cut in the circumferential direction, so we fixed it at both ends of the pipe ($U_1=U_2=U_3=0$, $UR_1=UR_2=UR_3=0$: displacement and rotation are blocked).

A load applied to the structure studied is represented by a pressure defined on the pipe's inner surface. The boundary conditions are presented in Figure 2.
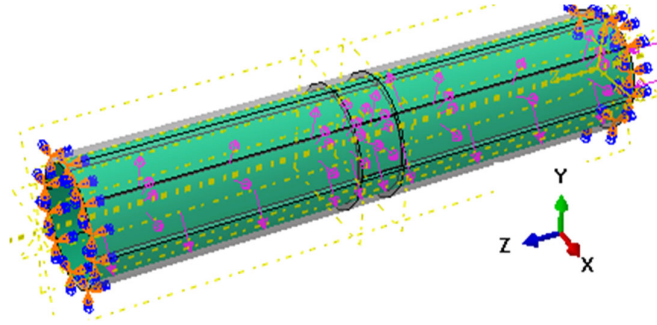
Figure 2 – Boundary conditions of the corroded pipe

Mesh model

The overall structure is based on a regular mesh for all calculations in this study. The mesh remains unchanged throughout the calculation to prevent any impact on the results, as shown in Figure 3. For the type of mesh elements, one was satisfied with the C3D8R elements, widely used in the modelling of these structures. The total number of nodes is 7660. The total number of the pipe elements is about 5010.
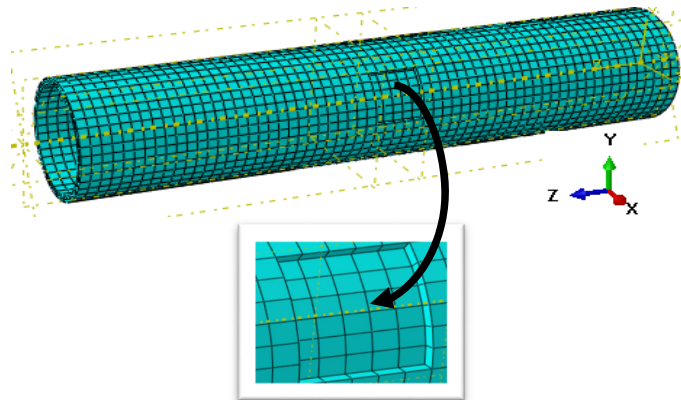

Figure 3 – Detailed mesh used for a numerical model of the corroded pipe

Convergence of the results

In finite element simulations, it is generally observed that using a more detailed mesh leads to more accurate results. Conducting mesh convergence research of this kind can provide a precise answer.

Furthermore, this paper aims to enhance the mesh density through a convergence study of the structure's density to strike a balance between computation time and desired accuracy.

Figure 4 illustrates the impact of changing the density of the mesh on the highest value of the von Mises constraint in the assembly. Based on Figure 4, a refined mesh leads to a higher value of the von Mises constraint. However, the von Mises value remains relatively constant if the mesh is adjusted to have a higher density across the structure.

The pipe dimensions were set as shown in Table 1 and the type of hexagonal linear meshing chosen. The number of finite elements was increased in order to refine the structure mesh from 1601 (less refined) to 33886 elements (very refined mesh) by using this technique in the Abaqus software, thanks to the options such as seed part instance, where the number of elements can be modified until achieving stability in the value of the von Mises stress.
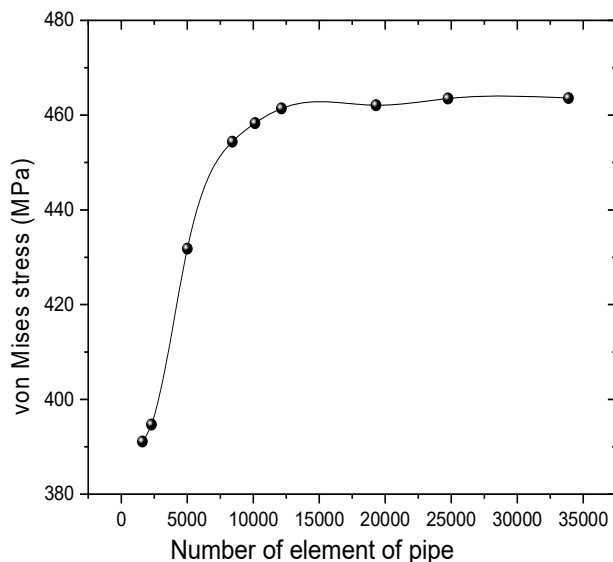

Figure 4 – Variation of von Mises stress as a function of the mesh density in the pipe for P=20MPa

Results and discussion

Model of burst pressure without defect

Burst pressure for intact pipelines

Some available approaches estimate burst pressure for free-defect pipes or with grooves with an infinite longitude. The approach of the von Mises is expressed as follows: (Amaya-Gómez et al, 2019)

$$P_b = \frac{4t\sigma_{uts}}{D}\left(\frac{k}{2}\right)^{n+1} \tag{1}$$

and

$$k = \frac{2}{\sqrt{3}}$$

where

P_b is the burst pressure,
σ_{uts} is the ultimate stress,
t is the pipe thickness, and
D is the Internal diameter.

Based on our finite element model, we have developed an analytical model for calculating burst pressure for an undamaged pipe; that is to say, the present model (equation 2) is obtained by the interpolation of the numerical results (FEM results), see Table 3, written as follows:

$$P_b = \frac{\sigma_{uts}}{n}\left(\frac{R_{ext}}{R_{int}}\right)\left(3,74325.10^{-5} + 0,00297\,t - 1,03764.10^{-4}\,t^2\right) \tag{2}$$

n: The hardening coefficient is equal to 0.127 for the used steel,

where

R_{ext} is the external radius of the pipe, and
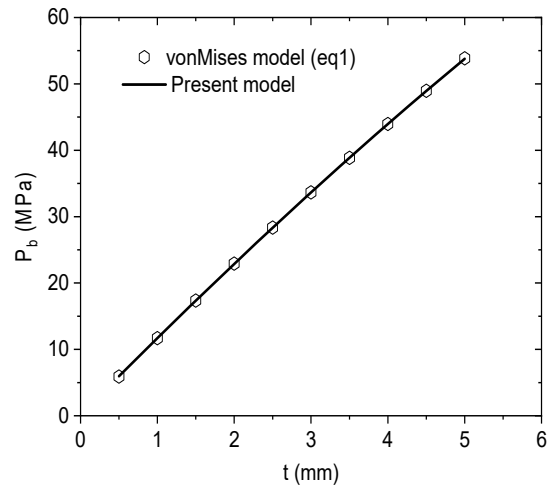R_{int} is the internal radius of the pipe.

Figure 5 – von Mises results compared with the present model

Figure 5 presents the von Mises results compared with the present model. The maximum and minimum variations are 0.6789% and 0.00043%, respectively (See Table 3). The analytical solution gives a good agreement of the burst pressure for intact pipelines compared with the von Mises results.

$$e(\%) = \left| \frac{P_b^{von\,Mises} - P_b^{present\,model}}{P_b^{von\,Mises}} \right| \times 100 \qquad (3)$$

Table 3 – von Mises results are compared to the current model

P_b (von Mises)	P_b (Present model)	e (%)
5.91698926	5.95716214	0.6789413
11.7053483	11.685805	0.16696062
17.3692265	17.3264919	0.24603626
22.9125967	22.8724143	0.17537247
28.3392643	28.3167635	0.07939824
33.6528764	33.6527307	0.00043289
38.8569294	38.8735074	0.04266414
43.9547773	43.9722849	0.0398309
48.9496384	48.9422545	0.0150846
53.8446022	53.7766076	0.12627935

Effect of internal pressure

This part of the work numerically analysed the effect of internal pressure applied to a pipeline bearing an external square defect centred on the level and distribution of stresses induced in this structure using the finite element method. The results obtained are illustrated in Figure 6. It shows the distribution and variation of equivalent von Mises stresses as a function of internal pressure. The stresses were computed along path one, as shown schematically in Figure 1b.

Evaluation of stresses along path 1

This study evaluated the equivalent and the internal stresses along path 1; the obtained results are shown in Figure 6. The stresses were computed along path 1.

The effect of internal pressure on the intensity of equivalent and normal stresses is illustrated in Figure 6. Increasing internal pressure increases the amplitude of this stress, which reaches its maximum at the centre of the defect. The von Mises stress reaches its maximum level ($\sigma \sim 280$MPa) at the defect located at the centre of the pipe with a pressure of 20MPa (Figure 6a).

The damage rate is equal to 60%. Even for internal normal stresses, radial stresses (Figure 6b) are almost half as high as von Mises stresses ($\sigma \sim 50$MPa) for an applied internal pressure of 20 MPa.

The distribution of circumferential stress (Figure 6c) is identical to that of von Mises stresses and at the same level, which is the highest. Longitudinal stresses increase with each applied pressure and reach the lowest level at the ends relative to the centre of the defect, as shown in Figure 6d.

Comparative analysis

This part of the work, a comparative study between a flawless pipe and a pipe with an external-centred cubic defect (a =40mm, b=40mm, and c=4mm), presents the von Mises stress induced in the two pipes studied, subjected to internal stresses (10-15-20MPa), to see the effect of the defect and internal pressure on the increase in stress intensities demanded in this no-defect pipe, see Figure 7.

The first point to note from this Figure is that these equivalent stress levels lead us to conclude that the pipeline with a defect, subjected to very high internal pressures, particularly at the defect centre (over 452 MPa 20MPa internal pressures), can lead to ruin and put these pipes out of service. On the other hand, the equivalent von Mises stresses of a defect-free pipeline are much lower (over 188 MPa at 20 MPa internal pressures). These observations conclude that the pipe bearing the external defect should be repaired with a composite casing to reduce and absorb these high stresses. The damage rate is equal to 46%.
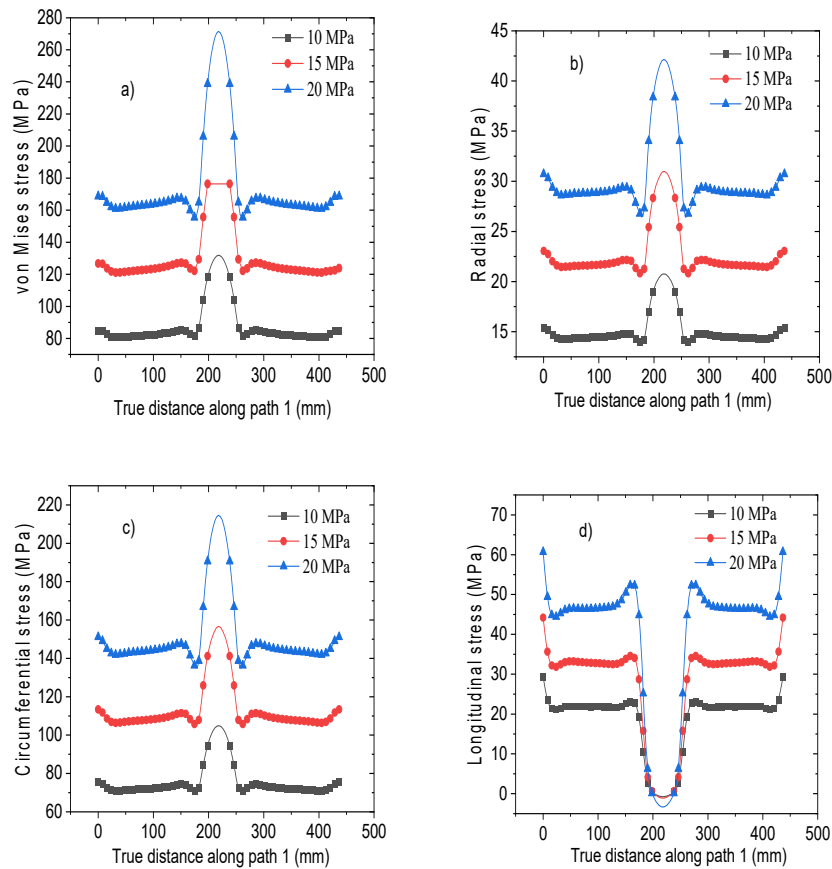

Figure 6 – von Mises and normal stress variation as a function of internal pressure along path 1
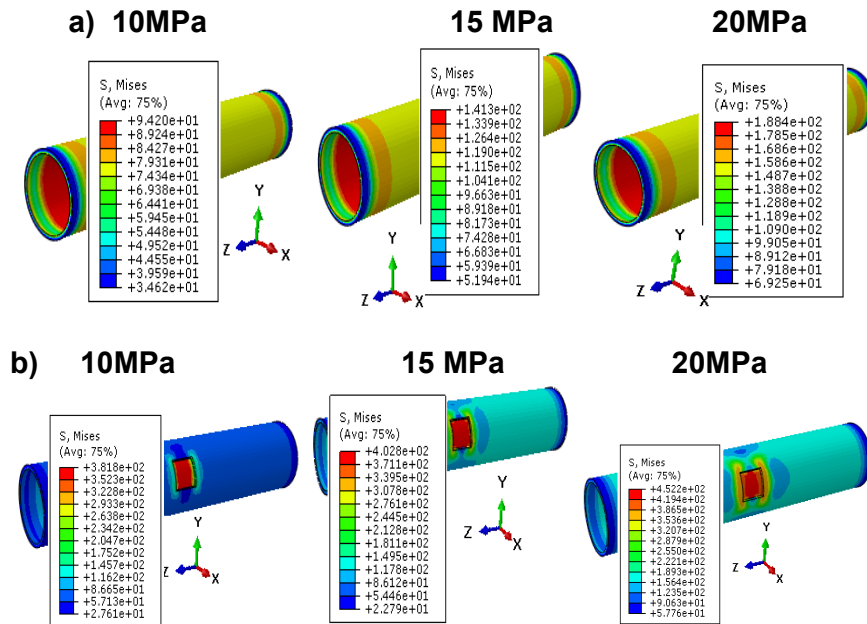
Figure 7 – von Mises equivalent stress level as a function of internal pressure: a) Pipe without defect, b) Pipe with defect

Depth and spacing effect

This part of the work will present the effect of the interaction of two centred cubic corrosion defects located outside the pipe on the level and distribution of equivalent stress generated in the pipeline as a function of defect depth and imposed internal pressure. Metehri et al. (2018) conducted almost the same study which determined the effect of two interactions on the stress intensity factors in S_iC particles reinforced Al composite.

It can be seen in Figure 8 that high stress occurs at the centre of the corrosion defect. The von Mises stress was calculated over a range of defect distances d=5-10-20-40-60 and 80mm and with varying defect depths c=1-2-3 and 4mm. The analysis by the finite element method of this Figure illustrates that the equivalent stress induced in the pipe, specifically in the defects, increases progressively as the distance between the two corrosion defects decreases (d=5mm). In other words, a decrease in the distance between square defects leads to an increase in the equivalent

stress, and this value is accentuated if the defect depth (c= 4mm) is too great about the thickness of the steel pipe itself. This behaviour constitutes a risk of the pipe bursting since it has exceeded the ultimate stress (σ_{uts}=500MPa) at internal pressure P=20MPa. The damage rate is equal to 50%. On the contrary, these stresses generally decrease if the distance between defects increases.
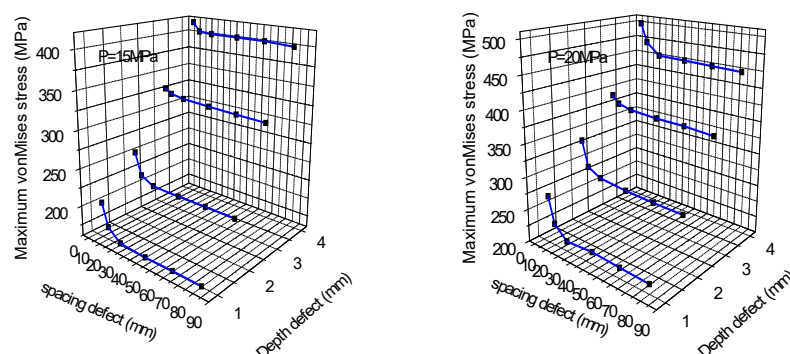

Figure 8 – Maximum von Mises stress variation in the pipe in correlation to the spacing and depth defect

Size effect

In the present study, the finite element method has been inserted to analyse the equivalent von stresses in three models of different sizes, but the same defect shape and the same depth defect (c=4mm). The first defect has the dimensions a=40mm, b=40mm; the second defect has the dimensions: a=50mm, b=50mm; the third defect has the dimensions: a=60mm, b=60mm, and, depending on the application, the internal pressure is from 15 to 20 MPa. The results were obtained by plotting the curves along path 1 (Figure 1b).

From these curves (Figure 9), the defect size considerably determines the level of equivalent stresses. As the defect size increases, the stress level automatically increases; always remember the effect of internal pressure. Equivalent stress values at internal pressure P=20MPa, whether path one and with large defect sizes, reach very high values, leading to catastrophic failure.
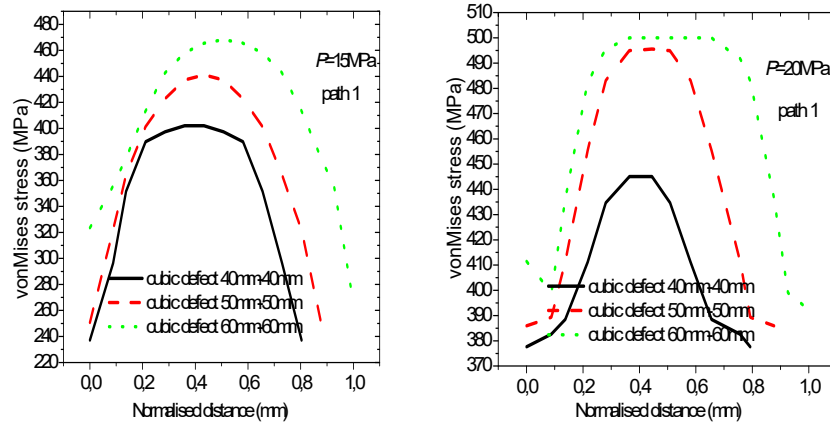
Figure 9 – von Mises stress variation in the pipe related to the size defect

Thickness and depth effect

Gas pipelines are constantly exposed to high internal pressure due to the transport of hydrocarbons. For this reason, it is strictly essential that special attention must be paid to a three-dimensional numerical study to analyse the geometric parameters of the cylindrical structure, including the effect of the pipeline radius and, therefore, its thickness, plus the fundamental parameter (defect depth) when the pipe carries defect to the outside. Two curves are plotted for this study for two values of internal pressure. The results are shown in Figure 10. This later shows the variation of the maximum von Mises stress related to the pipe thickness and defect depth, respectively. The analysis of this Figure shows that even if the pipe thickness is optimised (t=8mm), the equivalent stress value increases with increasing the defect depth value, exceeding the elastic limit, even the ultimate strength, especially at high pressure.

On the contrary, if the defect depth is minimal (c=1mm) and the pipe thickness is maximised (t=24mm), the equivalent stress values present no risk of damage. High internal pressures (P=20MPa) inducing high von Mises stress values should be avoided. As mentioned above, thick gas pipelines have good strength and resistance, firstly to high pressures and secondly to bursting, and guarantee good performance for this type of transport. However, it must be stressed that this geometric parameter

(thickness pipe) determines the rigidity of cylindrical structures. It is, therefore, advisable to use thick-walled pipelines with a minimum depth defect.
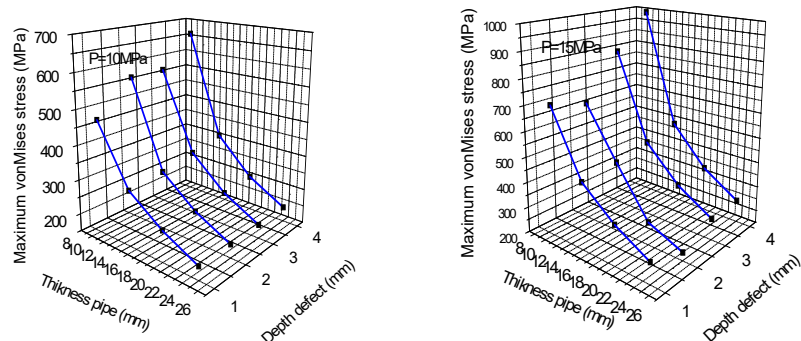

Figure 10 – Maximum von Mises stress variation in the pipe as a function of the thickness defect

Location effect

Cubic defect

This part of the work deals with the shape of a square corrosion defect of the dimensions a=40mm, b=40mm, and c=4mm. In the first case, this defect is located inside the centre of the cylindrical pipe, and in the second case, it is outside at the edges. This study aims to show the effect of the defect location on the variation and level of von Mises stress along path 1.

The analysis of Figure 11 by the finite element method shows that the equivalent stresses generated in a pipe by a square defect are generally of a higher level, mainly when the defect is located outside the edge, where these stresses reach ~440MPa if 20MPa of internal pressure is applied and a value that exceeds the elastic limit of steel. These stresses may present a high probability of pipe bursting. As a result, the equivalent stress values of a pipe with a square corrosion defect in the centre of the interior are correspondingly higher. Based on the results presented below, it is clear that pipelines with square defects, whether on the inside, inside edge, or in the centre, are at risk of ductile damage to the corroded pipe.
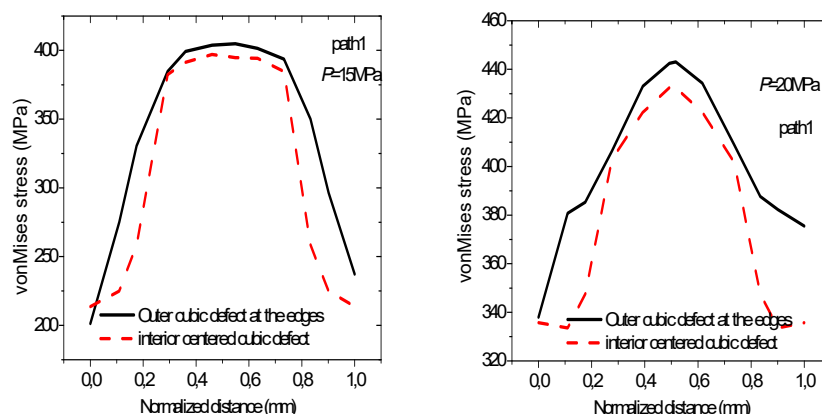
Figure 11 – von Mises stress variation in pipe as a function of the location of the cubic defect

Rectangular parallelepiped defect

In this study, it is also important to note that the rectangular parallelepiped corrosion defect of the dimensions a=40mm, b=60mm, and c=4mm generally located outside at the edges of the structure and inside at the centre, was chosen. This study by FEM analysis aims to determine the effect of the defect position on the variation and level of von Mises stresses along path 1.

The analysis of Figure 12 illustrates that the von Mises stresses generated by the rectangular parallelepiped defect are intensive and very high when positioned outside the pipe edge. They reach ~430MPa in case of the application of 15MPa of internal pressure, they reach more than 480 MPa, and in case of the application of 20MPa, this value exceeds the elastic limit of steel material and is close to the ultimate strength; the damage rate is equal to 50%. The higher these stresses, the greater the risk of pipe bursting. On the other hand, the equivalent stress values for a pipe with a rectangular parallelepiped corrosion defect in the centre of the interior present no risk of bursting. Based on the results presented below, it is clear that pipelines with rectangular defects in the centre and interior of the pipe are most often at risk of damage and reliability.
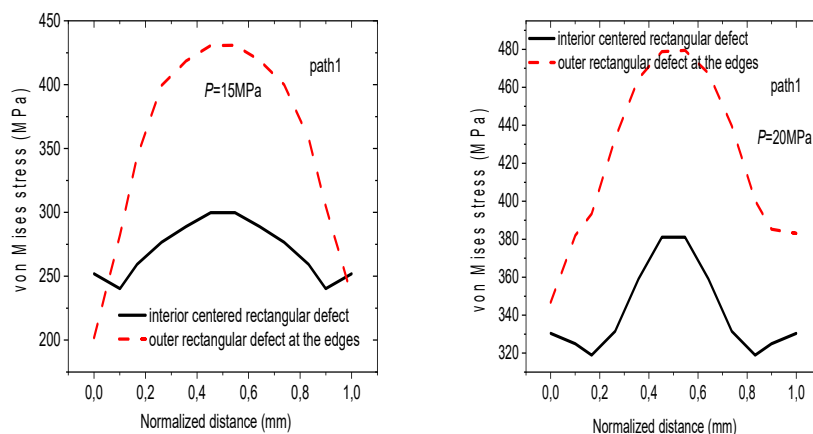
Figure 12 – von Mises stress variation in pipe as a function of the location of the rectangular defect

Shape effect

In this study, we wanted to numerically demonstrate the effect of the defect shape on the distribution and level of von Mises stresses. For this reason, we took samples of different defect shapes, provided the defect is located in the centre of the pipeline, with a maximum depth of 4mm. The dimensions for the cube-shaped defect were chosen to be a=40mm and b=40mm, for circular-shaped defects 2a= 8mm and 2b= 8mm, and for the elliptical-shaped defect 2a=40mm and 2b=8mm. The parallelepiped rectangle-shaped defects for the last sample were of the dimensions a=40 and b=70mm.

The results are shown in Figure 13. The latter shows the von Mises stress distribution according to path one at an internal pressure of 10 MPa, with different defect shapes and sizes. In the case of the circular defect, the maximum value of the equivalent stress, which is evenly distributed, remains at a low level of 200 MPa. When the defect becomes elliptical, there is a concentration of stress in the corners of the defect. In this case, the maximum equivalent stress exists at the pointed corner. It can reach 450 MPa, a value almost equal to the ultimate stress of steel (see Table 2), which is a higher level corresponding to just 10 MPa internal pressures and which can lead to damage to gas transport; the damage rate is equal to ∼ 45%. As a comparison between circular and elliptical defects, we can

see a difference of more than half in the very high level of the circular defect, which presents no risk of pipe bursting. The level of the cubic defect is 370 MPa, while the level of the rectangular parallelepiped defect is 384 MPa, which exceeds the material's elastic limit. The distribution and value of the equivalent stress in the flaw vary depending on the flaw shape and internal pressure. If the pressure is increased, the level of equivalent stress increases. The maximum equivalent plastic strain in steel bearing an elliptical-shaped defect is much higher than that in a pipe bearing a circular defect, where the strain is distributed uniformly around the defect.
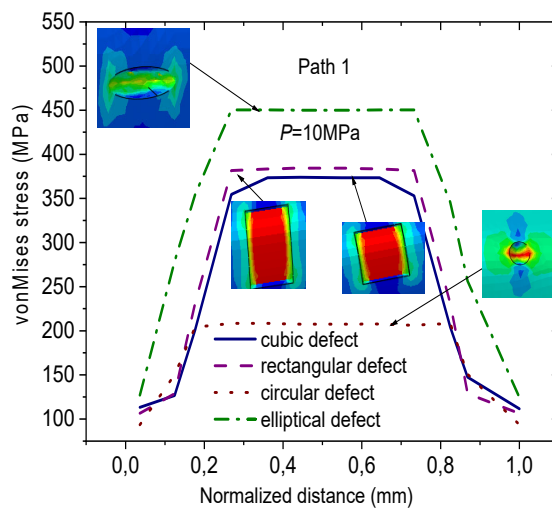

Figure 13 – von Mises stress variation in the pipe depending on the shape effect for P = 10MPa

Analytical model with the elliptical defect

From the above results (Figure 13), where the elliptical defect was found to have a very high level of von Mises stresses compared to other defects, we opted to perform an analytical validation in the case of a pipe with an elliptical defect. Therefore, an analytical model was developed to determine the bursting pressure for a pipe with an elliptical corrosion defect. The results of this model will be compared with those of the recalibrated PCORRC model. (Teoh et al, 2022).

Recalibrated PCORRC Model

Yeom et al. (2015) recalibrated the PCORRC model for X65 corroded pipes using full-scale test data and 3D FEA computations.

$$P_b = \frac{2t(0.9\sigma_{uts})}{D}\left(1-\frac{d}{t}\left(1-\exp\left(-0.224\frac{L}{\sqrt{D(t-d)/2}}\right)\right)\right). \qquad (4)$$

for $0.1\le$

$\frac{L}{\sqrt{Dt}} \le 12, 0.1 \le d \le 0.875$

where

D/t is the ratio of the defect, and

L is the length of the defect.

Lacking a defect, equation (4) reduces to $P_b = 0.9\sigma_{uts} \times (2t/D)$ for defect-free pipes. This model may also be conservative.

Present model

From the finite element results, the following model was extracted

$$P_b = \frac{2t(0.9\sigma_{uts})}{D}\left(A_0+A_1\exp\left(A_2\left(\frac{L}{\sqrt{Dt}}\right)\right)\right). \qquad (5)$$

for $0.1 \le \frac{L}{\sqrt{Dt}} \le 12, \ 0.1 \le d \le 0.875$

$$A_0= -8,8817.10^{-16}\left(\frac{d}{t}\right)^2 -\left(\frac{d}{t}\right)+1$$

$$A_1= 8,88178.10^{-16}\left(\frac{d}{t}\right)^2 +\left(\frac{d}{t}\right)+1.66533.10^{-16} \qquad (6)$$

$$A_2 = -1,17376\left(\frac{d}{t}\right)^2 +0,41926\left(\frac{d}{t}\right)-0,36419$$

where

t is the pipe thickness (mm),

d is the depth defect (mm), and

A_0, A_1, and A_2 are the Integration functions.

This model determines the variation of the burst pressure as a function of the geometrical parameters of the defect and the pipe. In the comparison between our model and the PCORRC model one (Figure 14), we can see an excellent agreement; the results of the two models are practically equal. This allows us to validate our model. The results

1764

presented in Table 4 consolidate this validation, as the maximum error between the two models does not exceed 0.3%.

Table 4 – Burst pressure results of the PCORRC model compared with the present model for the defect ratios defect (d/t=, and 0.8)

|	$0 \leq L/(Dt)^{0.5} \leq 12$								
	d/t=0.1			d/t=0.5			d/t=0.8		
$L/(Dt)^{0.5}$	Pb/Pbi (Present)	Pb/Pbi (PCORRC)	e (%)	Pb/Pbi (Present)	Pb/Pbi (PCORRC)	e (%)	Pb/Pbi (Present)	Pb/Pbi (PCORRC)	e (%)
0	1	1	$2,21.10^{-14}$	1	1	$2,22.10^{-14}$	1	1	$2,22.10^{-14}$
0,0365	0,9987	0,9987	$-2,037.10^{-4}$	0,9918	0,9918	$-1,73.10^{-4}$	0,9718	0,9718	$-6,59E^{-6}$
0,3651	0,9885	0,9885	$-1,702.10^{-4}$	0,9245	0,9245	$-4,08.10^{-4}$	0,7558	0,7558	$-1,55E^{-4}$
0,5477	0,9832	0,9832	$-8,272.10^{-4}$	0,8912	0,8912	$4,653.10^{-4}$	0,6606	0,6606	$4,73E^{-4}$
0,9128	0,9737	0,9737	$-0,00106$	0,8321	0,8321	$-1,81.10^{-4}$	0,5111	0,5111	$-6,75E^{-4}$
1,0954	0,9693	0,9693	$-1,588.10^{-4}$	0,8060	0,8060	$-2,76.10^{-4}$	0,4529	0,4529	$-3,81E^{-4}$
1,8257	0,9543	0,9543	$-4,243.10^{-4}$	0,7206	0,7206	$2,512.10^{-4}$	0,2954	0,2954	$-0,00103$
2,1908	0,9481	0,9481	$-4,091.10^{-4}$	0,6873	0,6873	$1,119.10^{-4}$	0,2478	0,2478	$-8,10E^{-4}$
3,2863	0,9333	0,9333	$-4,644.10^{-4}$	0,6147	0,6147	$1,4469E^{4}$	0,1711	0,1711	$-0,0015$
4,5643	0,9217	0,9217	$-7,610.10^{-4}$	0,5647	0,5647	$2,0734E^{4}$	0,1396	0,1396	$0,0014$
5,4772	0,9160	0,9160	$-9,904.10^{-4}$	0,5429	0,5429	$5,8709E^{-4}$	0,1314	0,1314	$-0,0026$
7,3029	0,9087	0,9087	$-7,671.10^{-4}$	0,5189	0,5189	$6,8554E^{-6}$	0,1262	0,1262	$-3,299E^{-4}$
9,1287	0,9047	0,9047	$6,774.10^{-4}$	0,5083	0,5083	$4,8104E^{-4}$	0,1252	0,1252	$-0,0037$
10,9541	0,9025	0,9025	$-4,064.10^{-4}$	0,5037	0,503	$-9,677E^{-4}$	0,1250	0,1250	$-0,0018$
	0,90182	0,90181	$7,6899.10^{-4}$	0,50231	0,5023	$0,0026$	0,12502	0,12502	$-0,00102$
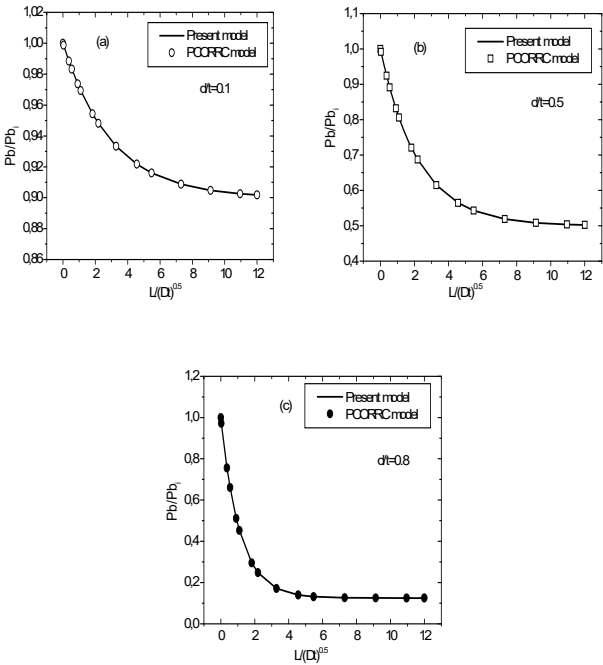
Figure 14 – Comparison of the burst pressure of the present model with the PCORRC model

Conclusions

This study examines the process of corrosion evaluation in order to identify the remaining structural integrity of thin-walled pipelines with corrosion problems. The objective is to develop a corrosion assessment model specifically tailored to analyse the effects of damage on pipes under internal pressure. This study employed the finite element approach to conduct an analytical and numerical investigation of a pipe. The objective was to construct models that can accurately estimate the burst pressure of defect-free straight pipes using mathematical extrapolation. This paper discusses the impact of several factors on the integrity of pipes, including the depth of flaws, the pipe thickness, the form, the size, the position, the distance between corrosion defects, the interaction between internal and exterior defects, and the influence of external defects on the overall integrity. This study enables assessing the damage rates of all flaws more accurately, considering other parameters such as internal pressure. The research introduces a novel model that accurately forecasts the burst pressure of a flawed straight pipe. This prediction holds immense importance for structural design and safety evaluation. The obtained results are compared with those of the PCORRC model, and the presented model aligns with the analytical solution found in the literature. Future research will focus on analysing the fluctuation of burst pressure in corroded pipes that have been repaired using bonded composite wrap.

References

Abyani, M., Bahaari, M.R., Zarrin, M. & Nasseri, M. 2022. Predicting failure pressure of corroded offshore pipelines using an efficient finite element-based algorithm and machine learning techniques. *Ocean Engineering*, 254, art.number:111382. Available at: https://doi.org/10.1016/j.oceaneng.2022.111382.

Amaya-Gómez, Sánchez-Silva, M., Bastidas-Arteaga, E., Schoefs, F. & Muñoz, F. 2019. Reliability assessments of corroded pipelines based on internal pressure – A review. *Engineering Failure Analysis*. 98, pp.190-214. Available at: https://doi.org/10.1016/j.engfailanal.2019.01.064.

-ASME. 2012. *B31 - Manual for Determining the Remaining Strength of Corroded Pipelines* [online]. Available at: https://www.asme.org/codes-standards/find-codes-standards/b31g-manual-determining-remaining-strength-corroded-pipelines/2012/pdf [Accessed: 09 April 2024]. ISBN: 978079183448.

Deng, K., Yang, P., Bing, L., Lin, Y. & Jiandong, W. 2021. Through-wall yield ductile burst pressure of high-grade steel tube and casing with and without corroded defect. *Marine Structures*, 76, art.number:102902. Available at: https://doi.org/10.1016/J.Marstruc.2020.102902.

-DNV. 2021. *DNV-RP-F101 Corroded pipelines, Recommended practice, Edition 2019-09 - Amended 2021-09*. *dnv.com* [online]. Available at: https://www.dnv.com/oilgas/download/dnv-rp-f101-corroded-pipelines/
[Accessed: 09 April 2024].

Fezazi, A.I., Mechab, B., Salem, M. & Serier, B. 2021. Numerical prediction of the ductile damage for axial cracks in pipe under internal pressure. *Frattura ed Integrità Strutturale*, 15(58), pp.231-241. Available at: https://doi.org/10.3221/IGF-ESIS.58.17.

Guidara, M.A., Bouaziz, M.A., Dallali, M., Schmitt. C., Haj Taieb, E. & Azari, Z. 2018. HDPE Pipe Failure Analysis Under Over pressure in Presence of Defect. In: Haddar, M., Chaari, F., Benamara, A., Chouchane, M., Karra, C. & Aifaoui, N. (Eds.) *Design and Modeling of Mechanical Systems—III. CMSM 2017. Lecture Notes in Mechanical Engineering,* pp.1027-1038. Cham: Springer. Available at: https://doi.org/10.1007/978-3-319-66697-6_101.

-Hibbitt, Karlsson & Sorensen, Inc. 2014. *ABAQUS/CAE, User's Manual, Ver 6.14*. Hibbitt, Karlsson & Sorensen, Inc.

Jiang, F. & Zhao, E. 2022. An integrated risk analysis model for corroded pipelines subjected to internal pressures: Considering the interacting effects. *Ocean Engineering*, 247, art.number:110683. Available at: https://doi.org/10.1016/j.oceaneng.2022.110683.

Mechab, Be,. Chioukh, N., Mechab, Bo. & Serier, B. 2018. Probabilistic Fracture Mechanics for Analysis of Longitudinal Cracks in Pipes under Internal Pressure. *Journal of Failure Analysis and Prevention*, 18, pp.1643-1651. Available at: https://doi.org/10.1007/S11668-018-0564-8.

Mechab, B., Salem, M., Medjahdi, M. & Serier, B. 2020. Probabilistic Elastic-plastic Fracture Mechanics Analysis of Propagation of Cracks in Pipes under Internal Pressure. *Frattura ed Integrità Strutturale*,14(54), pp.202-210. Available at: https://doi.org/10.3221/IGF-ESIS.54.15.

Mechab, B., Serier, B., Bachir Bouiadjra, B.A., Kaddouri, K. & Feaugas, X. 2011. Linear and non-linear analyses for semi-elliptical surface cracks in pipes under bending. *International Journal of Pressure Vessels and Piping*, 88(1), pp.57-63. Available at: https://doi.org/10.1016/J.Ijpvp.2010.11.001.

Mechab, B., Serier, B., Kaddouri, K., Bachir Bouiadjra, B.A. 2014. Probabilistic elastic plastic analysis of cracked pipes subjected to internal pressure loads. *Nuclear Engineering and Design*, 275, pp.281-286. Available at: https://doi.org/10.1016/j.nucengdes.2014.05.008.

Metehri, A., Madani, K. & Lousdad, A. 2018. Effect of crack position and size of particle on SIF in SiC particles reinforced Al composite. *Frattura ed Integrità Strutturale*, 13(48), pp.152-160. Available at: https://doi.org/10.3221/IGF-ESIS.48.18.

Muthanna, B.G.N., Bouledroua, O., Meriem-Benziane, M., Razavi Setvati, M. & Djukic, M.B. 2021. Assessment of corroded API 5L X52 pipe elbow using a modified failure assessment diagram. *International Journal of Pressure Vessels and Piping*, 190, art.number:104291. Available at: https://doi.org/10.1016/J.Ijpvp.2020.104291.

Salem, M., Mechab, B., Berrahou, M., Bachir Bouiadjra, B.A. & Serier, B. 2019. Failure Analyses of Propagation of Cracks Repaired Pipe Under Internal Pressure. *Journal of Failure Analysis and Prevention,* 19, pp.212-218. Available at: https://doi.org/10.1007/s11668-019-00592-3.

Teoh, C.Y., Pang, J.S., Abdul Hamid, M.N, Ooi, L.E. & Tan, W.H. 2022. Ultrasonic guided wave testing on pipeline corrosion detection using torsional T(0,1) guided waves. *Journal of Mechanical Engineering and Sciences (JMES)*, 16(4), pp.9157-9166. Available at: https://doi.org/10.15282/jmes.16.4.2022.01.0725.

Wang, Z., Zhou, Z., Xu, W., Yang, L., Zhang, B. & Li, Y. 2020. Study on inner corrosion behavior of high strength product oil pipelines. *Engineering Failure Analysis*, 115, art.number:104659. Available at: https://doi.org/10.1016/J.Engfailanal.2020.104659.

Yeom, K.J., Lee. Y.-K., Oh, K.H. & Kim, W.S. 2015. Integrity assessment of a corroded API X70 pipe with a single defect by burst pressure analysis. *Engineering Failure Analysis*, 57, pp.553-561. Available at: https://doi.org/10.1016/J.Engfailanal.2015.07.024.

Yi, S., Xiao, Z., Can, F., Junyan, H. & Cheng, Y.F. 2022. A novel model for prediction of burst capacity of corroded pipelines subjected to combined loads of bending moment and axial compression. *International Journal of Pressure Vessels and Piping*, 196, art.number:104621. Available at: https://doi.org/10.1016/J.Ijpvp.2022.104621.

Zelmati, D., Bouledroua, O., Hafsi, Z. & Djukic, M.B. 2020. Probabilistic analysis of corroded pipeline under localised corrosion defects based on the intelligent inspection tool. *Engineering Failure Analysis*, 115, art.number:104683. Available at: https://doi.org/10.1016/j.engfailanal.2020.104683.

Zhao, J., Lv, Y. & Cheng, Y.F. 2022. A new method for assessment of burst pressure capacity of corroded X80 steel pipelines containing a dent. *International Journal of Pressure Vessels and Piping*, 199, art.number:104742. Available at: https://doi.org/10.1016/j.ijpvp.2022.104742.

Zhou, W., Bao, J., Cui, X.Z. & Hong, H.P. 2021. Modeling and simulating non homogeneous non-Gaussian corrosion fields on buried pipelines and its use in predicting burst capacities of corroded pipelines. *Engineering Structures*, 245, art.number:112957. Available at: https://doi.org/10.1016/j.engstruct.2021.112957.

Zhuwu, Z., Liping, G. & Cheng, Y.F. 2020. Interaction betweeninternal and externaldefects on pipelines and its effect on failure pressure. *Thin-Walled Structures*, 159, art.number:107230. Available at: https://doi.org/10.1016/J.Tws.2020.107230.

Una nueva investigación utilizada para predecir la presión de la explosión en tuberías rectas corroídas bajo presión interna

Aicha Metehri*, **autor de correspondencia***,
Belaïd Mechab*, Bel Abbes* Bachir Bouiadjra

Universidad de Sidi Bel Abbes, Facultad de Tecnología, Departamento de Ingeniería Mecánica, Laboratorio de Mecánica Física de Materiales, Sidi Bel Abbès, República Argelina Democrática y Popular

Resumen:

Introducción/objetivo: Existe un interés creciente en la integridad de las tuberías y sus efectos en los aspectos económicos y de seguridad. Este estudio examina el proceso de evaluación de la corrosión para identificar la integridad estructural restante de tuberías de paredes delgadas con problemas de corrosión.

Métodos: Este trabajo tiene como objetivo crear un modelo de evaluación de la corrosión que pueda analizar el deterioro de tuberías de acero causado por la presión interna. Un estudio utilizó el enfoque de elementos finitos para construir modelos para predecir la presión de rotura de tuberías rectas sin defectos. El estudio involucró análisis analítico y numérico y utilizó el método de extrapolación matemática.

Resultados: Este artículo discute el impacto de varios factores en la integridad de una tubería, incluida la profundidad de los defectos, el espesor de la tubería, la forma, el tamaño y la posición de las fallas, así como la interacción entre los defectos internos y externos. Adicionalmente, se discute la influencia de los defectos externos en la integridad general.

Conclusión: Se concluye que el modelo del criterio de falla por corrosión de tuberías (PCORRC) y el modelo presentado se alinean con la solución analítica documentada en la bibliografia. Esto tiene una inmensa importancia en el campo del diseño estructural y la evaluación de la seguridad.

Palabras claves: defecto de corrosión, tubería de acero, presión interna, falla, tensión, modelado.

Новейшие испытания, используемые для прогнозирования давления разрыва в прямых корродированных трубах под внутренним давлением

Айша Метехри, **корреспондент**,
Белаид Мехаб*, Бел Аббас* Башир Буяжра
Университет Сиди Бель-Аббес, технологический факультет,
Кафедра машиностроения,
Лаборатория физической механики материалов,
г. Сиди Бель-Аббес, Народная Демократическря Республика Алжир

Резюме:

Введение/цель: С каждым днем возрастает интерес к целостности трубопроводов и ее влиянию на экономические аспекты и безопасность. В данном исследовании рассматривается процесс оценки коррозии с целью выявления остаточной структурной целостности тонкостенных корродирующих трубопроводов.

Методы: Целью данной статьи является создание модели оценки коррозии, анализирующей износ стальных труб, вызванный внутренним давлением. В данном исследовании использовался метод конечных элементов в разработке моделей для прогнозирования давления разрыва неповрежденных прямых труб. В исследовании также применялись аналитический и численный анализы и метод математической экстраполяции.

Результаты: В статье рассматривается влияние нескольких факторов на целостность трубы, включая глубину повреждений, толщину трубы, форму, размер и расположение дефектов, а также взаимодействие между внутренними и внешними повреждениями. Кроме того, обсуждается влияние внешних повреждений на общую целостность трубопровода.

Вывод: В заключении сделан вывод о том, что модель критерия разрушения трубопровода вследствие коррозии (PCORRC) и представленная модель соответствуют аналитическому решению, описанному в существующей литературе. Результаты исследования представляют огромную значимость в области проектирования конструкций и оценки безопасности.

Ключевые слова: коррозионный дефект, стальная труба, внутреннее давление, разрушение, напряжение, моделирование.

Ново испитивање коришћено за предвиђање притиска прскања праве коридиране цеви под унутрашњим притиском

Ајша Метери, **аутор за преписку**,
Белаид Мехаб, *Бел Абас* Башир Бујажра

Универзитет Сиди Бел Абес, Технолошки факултет,
Одсек машинства, Лабораторија за физичку механику материјала,
Сиди Бел Абес, Народна Демократска Република Алжир

ОБЛАСТ: механика
КАТЕГОРИЈА (ТИП) ЧЛАНКА: оригинални научни рад

Сажетак:

Увод/циљ: Све је веће интересовање за интегритет цевовода као и за његов ефекат на економске и сигурносне аспекте. У овој студији испитује се процес процене корозије ради идентификације преосталог структурног интегритета коридираних танкозидних цевовода.

Методе: Креиран је модел евалуације корозије који може да анализира детериорацију челичних цеви услед унутрашњег притиска. Коришћен је приступ коначних елемената ради израде модела за предвиђање притиска прскања правих цеви без дефеката. Примењена је аналитичка и нумеричка анализа, као и математички метод екстраполације.

Резултати: Рад приказује утицај неколико фактора на интегритет цеви као што су дубина дефекта, дебљина цеви, облик, величина и позиција дефекта, као и међусобни утицај унутрашњих и спољашњих дефеката. Приказан је и утицај спољашњих дефеката на свеукупни интегритет.

Закључак: Закључује се да се модел критеријума лома цеви услед корозије (PCORRC) и модел представљен у овој студији подударају са аналитичким решењем из литературе. То има огроман значај у области пројектовања конструкција и процене сигурности.

Кључне речи: дефекат корозије, челична цев, унутрашњи притисак, лом, напон, моделовање.